Available online at www.sciencedirect.com

ScienceDirect

Procedia CIRP 46 (2016) 537 – 540

www.elsevier.com/locate/procedia

7th HPC 2016 – CIRP Conference on High Performance Cutting

Application of substructure decoupling techniques to predict mobile machine tool dynamics: Numerical investigations

Mohit Law[a], Hendrik Rentzsch[b]*, Steffen Ihlenfeldt[b,c] and Matthias Putz[b]

[a]*Indian Institute of Technology, Kanpur, India*
[b]*Fraunhofer Institute for Machine Tools and Forming Technology IWU, Chemnitz 09126, Germany*
[c]*Institute of Machine Tools and Control Engineering, Technische Universität Dresden, Germany*

* Corresponding author. Tel.: +49-371-5397-1392; fax: +49-371-5396-1392. *E-mail address:* hendrik.rentzsch@iwu.fraunhofer.de

Abstract

In situ machining of large workpieces is made possible by moving mobile machines to workpiece locations. To guide and enhance on site machining performance, dynamics of the assembled system must be predicted beforehand. Beforehand prediction of assembled response requires dynamics of the mobile machine in its free-free configuration be coupled with response of base/workpiece measured at location. Since obtaining the free-free response of the machine is non-trivial, this paper presents a substructure decoupling scheme that instead extracts the machine's response from known dynamics of the machine mounted on a base, and from information of a substructural base system. Simulation driven investigations show the decoupling scheme to be robust even under the vagaries of measurement noise and changes in the residual substructural base system. Extracted dynamics of the machine can be subsequently synthesized with known dynamics of other bases/workpieces for a priori prediction of assembled dynamics to guide first-time-right on site machining.

Peer-review under responsibility of the International Scientific Committee of 7th HPC 2016 in the person of the Conference Chair Prof. Matthias Putz

Keywords: Dynamics; Machine tool; Simulation; Mobile machine; Substructure decoupling

1. Introduction

Transporting mobile machine tools to workpiece locations makes it possible to manufacture these parts directly at the site of operation [1]. Modular concepts allow the machine to be placed locally at the workpiece, either by mounting the machine directly on the workpiece, or by mounting the machine on the ground, or on separate base/intermediate frames. Despite this versatility, every new workpiece/location results in different machine-workpiece system dynamics. These changing dynamics influence the machining- and control stability of the system. To guide first-time-right solutions, it hence becomes necessary to evaluate assembled system dynamics before moving the machine to the workpiece location.

A priori prediction of assembled dynamics involves combining the dynamics of the mobile machine in its unsupported free-free configuration with the dynamics of the workpiece/base measured on site. This problem, akin to a substructuring problem, consists of constructing models of large and complex systems by assembling the dynamics of its simpler components [2-3]. Substructuring hinges on being able to obtain the response of individual subsystems. Dynamics for an arbitrary workpiece/base that the machine is moved to can be obtained by direct on site measurements. However, obtaining the machine's dynamics in its free-free configuration is non-trivial and needs special test rigs.

To avoid the need for special test rigs, it is demonstrated in this paper, on a 5 strut parallel kinematic mobile machine tool available at Fraunhofer IWU, that it is instead possible to extract the machine's free-free response using substructure decoupling schemes. The decoupling problem as illustrated in Fig. 1 allows extracting the dynamics of the machine, i.e. of subsystem A, from known dynamics of the base, i.e. subsystem B, and from known assembled system dynamics of the machine on a base, i.e. system AB.

Peer-review under responsibility of the International Scientific Committee of 7th HPC 2016 in the person of the Conference Chair Prof. Matthias Putz
doi:10.1016/j.procir.2016.04.126

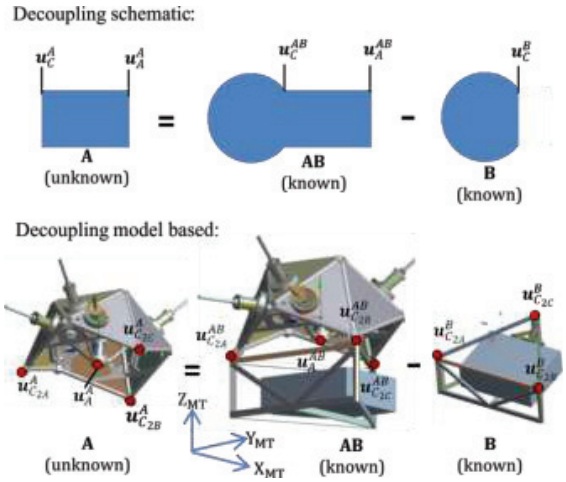

Fig. 1. Substructure decoupling scheme. Subsystem A corresponds to the machine, subsystem B corresponds to the residual substructural base system, and system AB corresponds to the machine mounted on the base.

Decoupling is formulated in Section 2 using the frequency based substructuring (FBS) method that uses frequency response functions (FRFs) of the (sub)systems [4]. The FBS based formulations are the preferred choice since FRFs of subsystems are relatively easy to obtain using measurements, and because a class of these FBS methods, referred to as the receptance coupling substructure analysis (RCSA) methods, has already found much use in machine tool applications for predicting tool point dynamics [5-7], and also in joint identification [8], and in extraction of rotational FRFs using the inverse RCSA approach [6, 8].

Though the decoupling scheme is intended to be used with measured system dynamics, discussions herein are limited to demonstrating the approach using virtual model(s) response only. FRFs to be used in decoupling are all obtained from finite element (FE) models of the base system and of the machine in the assembled configuration. Substructuring using these FRFs is carried out in the MATLAB environment. Extracted dynamics are verified in Section 3 against the free-free responses of the machine which are also obtained from the FE environment. Sensitivity of the extracted machine dynamics to noise and to changes in the substructural base system is investigated.

2. Substructure decoupling

The machine is mounted on the base at three connection points as shown in Fig. 1. Extracted dynamics include dynamics at these points and at the main point of interest, i.e. the spindle nose (point $\boldsymbol{u}_A^A$). To obtain these dynamics, the decoupling problem is formulated as one of finding the behavior of subsystem A that is part of the assembled system AB when additional opposing forces are applied at the interfaces, such that subsystem A experiences no connection forces from subsystem B [4].

With the dynamics of AB and B obtained by FE simulation, a dynamic stiffness representation of the system AB is:

$$\boldsymbol{Z}^{AB}\boldsymbol{u}^{AB} = \boldsymbol{f}^{AB} - \boldsymbol{g}^{AB} \tag{1}$$

and for subsystem B is:

$$\boldsymbol{Z}^{B}\boldsymbol{u}_C^B = \boldsymbol{f}_C^B + \boldsymbol{g}_C^B \tag{2}$$

wherein $\boldsymbol{u}^{AB} = \{\boldsymbol{u}_A^{AB};\ \boldsymbol{u}_C^{AB};\}^T$ comprises the vector sets of degrees of freedom (DoFs) at the spindle nose, i.e. $\boldsymbol{u}_A^{AB}$, and the vector sets of DoFs at all of the three coupling points, i.e. $\boldsymbol{u}_C^{AB} = \{\boldsymbol{u}_{C_{2A}}^{AB};\ \boldsymbol{u}_{C_{2B}}^{AB};\ \boldsymbol{u}_{C_{2C}}^{AB}\}^T$. Subscripts C and A denote coupling and spindle points respectively. Superscripts AB and B denote the assembled system and the subsystem respectively. Similarly, $\boldsymbol{u}_C^B$ is the vector set of DoFs at the three coupling points of the subsystem B, i.e. $\boldsymbol{u}_C^B = \{\boldsymbol{u}_{C_{2A}}^B;\ \boldsymbol{u}_{C_{2B}}^B;\ \boldsymbol{u}_{C_{2C}}^B\}^T$. $\boldsymbol{Z}^*$ represents the dynamic stiffness matrices. $\boldsymbol{f}^*$ has the same structure as $\boldsymbol{u}^*$, and represents the external force vectors at the corresponding DoFs in the assembled configurations of each (sub)system. The vector $\boldsymbol{g}^*$, like $\boldsymbol{f}^*$ represents the disconnection forces felt from the (de)coupling of the adjacent subsystems. Each of the vectors within the set of $\boldsymbol{u}^*$, $\boldsymbol{f}^*$ and $\boldsymbol{g}^*$represents the displacements and forces in each of the principal x, y, z directions respectively. Explicit direction and frequency dependency of terms in Eq. (1-2) are omitted for clarity.

Assuming rigid contact, the interface DoFs at matching coupling pairs must have the same displacements, i.e.:

$$\boldsymbol{u}_C^{AB} = \boldsymbol{u}_C^B. \tag{3}$$

These compatibility conditions of Eq. (3) can be rewritten compactly using a Boolean matrix description as:

$$\boldsymbol{B}\boldsymbol{u} = [\boldsymbol{B}^{AB} \quad \boldsymbol{B}^{B}]\begin{Bmatrix}\boldsymbol{u}^{AB}\\ \boldsymbol{u}_C^B\end{Bmatrix} = \boldsymbol{0} \tag{4}$$

wherein $\boldsymbol{B}$ extracts the coupling DoFs from among the full set of DoFs. The 'standard decoupling' formulations [4] are employed, which require that compatibility and equilibrium be satisfied only at the interface DoFs between subsystem B and the assembled system, AB.

Equilibrium conditions for an external force $\boldsymbol{f}_A^{AB}$ applied at $\boldsymbol{u}_A^{AB}$ results in interface forces balancing each other, i.e.:

$$\boldsymbol{g}_C^{AB} + \boldsymbol{g}_C^B = \boldsymbol{0}. \tag{5}$$

Rewriting Eq. (5) also with a Boolean matrix results in:

$$\boldsymbol{L}^T\boldsymbol{g} = [\boldsymbol{L}^{AB^T} \quad \boldsymbol{L}^{B^T}]\begin{Bmatrix}\boldsymbol{g}^{AB}\\ \boldsymbol{g}_C^B\end{Bmatrix} = \boldsymbol{0} \tag{6}$$

wherein $\boldsymbol{L}$ represents the nullspace of $\boldsymbol{B}$ or vice versa i.e. $\boldsymbol{L} = \text{null}(\boldsymbol{B})$, or $\boldsymbol{B}^T = \text{null}(\boldsymbol{L}^T)$ [4].

Employing the dual formulation for decoupling [4, 9], the interface forces are satisfied a priori. Substituting a form of Eq. (6) in Eq. (1-2) and also accounting for the compatibility in Eq. (4), the extracted mobile machine response can be shown in a compact matrix form as [9]:

$$[\boldsymbol{H}^A] = \begin{bmatrix}\boldsymbol{H}^{AB} & \boldsymbol{0}\\ \boldsymbol{0} & -\boldsymbol{H}^B\end{bmatrix} - \begin{bmatrix}\boldsymbol{H}^{AB} & \boldsymbol{0}\\ \boldsymbol{0} & -\boldsymbol{H}^B\end{bmatrix}\begin{bmatrix}\boldsymbol{B}^{AB^T}\\ \boldsymbol{B}^{B^T}\end{bmatrix} \times \left([\boldsymbol{B}^{AB} \quad \boldsymbol{B}^B]\begin{bmatrix}\boldsymbol{H}^{AB} & \boldsymbol{0}\\ \boldsymbol{0} & -\boldsymbol{H}^B\end{bmatrix}\begin{bmatrix}\boldsymbol{B}^{AB^T}\\ \boldsymbol{B}^{B^T}\end{bmatrix}\right)^{-1} \times [\boldsymbol{B}^{AB} \quad \boldsymbol{B}^B]\begin{bmatrix}\boldsymbol{H}^{AB} & \boldsymbol{0}\\ \boldsymbol{0} & -\boldsymbol{H}^B\end{bmatrix} \tag{7}$$

wherein FRF matrices $\boldsymbol{H}^{AB}$ and $\boldsymbol{H}^B$ are introduced in place

of the dynamic stiffness matrices $\boldsymbol{Z}^{AB^{-1}}$ and $\boldsymbol{Z}^{B^{-1}}$. Eq. (7) shows that the decoupling problem is equivalent to assembly of a negative dynamic stiffness for the substructure that one wants to subtract, i.e. $\boldsymbol{H}^{B}$ in the present case. $\boldsymbol{H}^{AB}$ within Eq. (7) takes the form of:

$$[\boldsymbol{H}^{AB}] = \begin{bmatrix} \boldsymbol{H}_{11}^{AB} & \boldsymbol{H}_{12A}^{AB} & \boldsymbol{H}_{12B}^{AB} & \boldsymbol{H}_{12C}^{AB} \\ & \boldsymbol{H}_{2A2A}^{AB} & \boldsymbol{H}_{2A2B}^{AB} & \boldsymbol{H}_{2A2C}^{AB} \\ & & \boldsymbol{H}_{2B2B}^{AB} & \boldsymbol{H}_{2B2C}^{AB} \\ sym & & & \boldsymbol{H}_{2C2C}^{AB} \end{bmatrix} \quad (8)$$

wherein $\boldsymbol{H}_{11}^{AB}$ corresponds to the receptance matrix at the spindle nose; $\boldsymbol{H}_{12A}^{AB}$ ... $\boldsymbol{H}_{12C}^{AB}$ correspond to the cross receptance matrices between the spindle nose and each of the three different coupling points. All other receptance matrices in Eq. (8) correspond to direct and cross receptance matrices between all of the three different coupling points in the assembled configuration.

Similarly, $\boldsymbol{H}^{B}$ within Eq. (7) consists of the direct and cross receptance matrices between all of the three different coupling points for only the residual subsystem B:

$$[\boldsymbol{H}^{B}] = \begin{bmatrix} \boldsymbol{H}_{2A2A}^{B} & \boldsymbol{H}_{2A2B}^{B} & \boldsymbol{H}_{2A2C}^{B} \\ & \boldsymbol{H}_{2B2B}^{B} & \boldsymbol{H}_{2B2C}^{B} \\ sym & & \boldsymbol{H}_{2C2C}^{B} \end{bmatrix}. \quad (9)$$

Each of the receptance matrices within Eq. (7-9) can be represented by direct and cross receptances in each of the principal axis as:

$$\boldsymbol{H} = \begin{bmatrix} h_{xx} & h_{xy} & h_{xz} \\ & h_{yy} & h_{yz} \\ sym & & h_{zz} \end{bmatrix} \quad (10)$$

wherein h represents the displacement-to-force receptance constructed using the mass normalized eigenvectors output from the FE environment:

$$h_{ij}(\omega) = \sum_{r}^{N_m} \frac{\Phi_{i_r}\Phi_{j_r}}{-\omega^2 + i_m 2\zeta_r \omega\omega_{n_r} + \omega_{n_r}^2} \quad (11)$$

wherein ω_n is the undamped eigenvalue for r modes of interest for a total of N_m modes; $\Phi_{i,j}$ is the eigenvector at the point of interest (i and j are the respective response and excitation points); ζ_r is the modal damping ratio; ω is the frequency vector and i_m is the imaginary operator.

All receptance matrices in Eq. (7-10) are symmetric, assuming reciprocity. Using the dual formulation for decoupling [9], the rows and columns corresponding to the coupling DoFs appear twice in $\boldsymbol{H}^{A}$, and only the independent entries need to be retained.

3. Decoupling results

Decoupled mobile machine tool dynamics (FRFs) calculated using Eq. (7) are compared in Fig. 2 with the unsupported free-free response of the mobile machine obtained from the FE environment. Response (FRF) comparisons are limited to the main point of interest, i.e. the spindle nose $\boldsymbol{u}_A^A$. Comparisons in Fig. 2 are also limited to response h_{xx} and h_{yy}, representing the main X_{MT} and Y_{MT} machine tool principal directions.

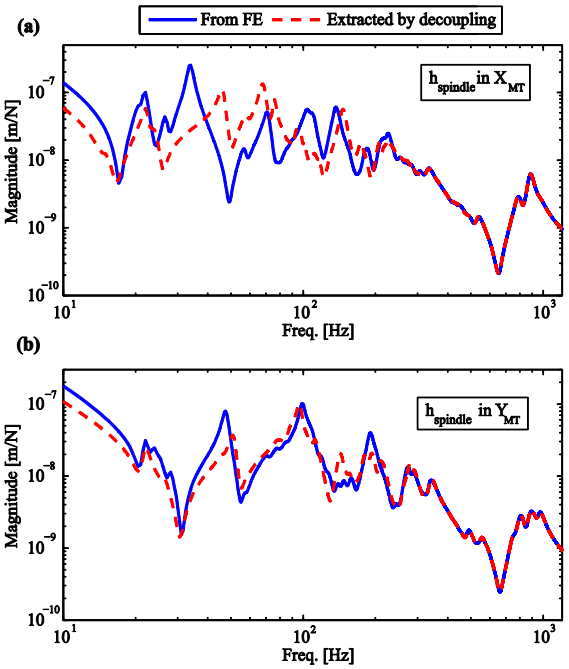

Fig. 2. Comparison of decoupled machine dynamics (FRFs) at the spindle nose with machine's free-free response obtained from the FE model. (a) Response in the X_{MT} direction. (b) Response in the Y_{MT} direction

As evident in Fig. 2, the calculated dynamics can, with the exception of some low-frequency modes in the X_{MT} direction, approximate the 'exact' dynamics obtained from the FE model reasonably well. Calculated dynamics in the Y_{MT} direction approximate the 'exact' trend rather well. Discrepancies in the X_{MT} direction, especially in the 30 – 100 Hz range can be attributed to known issues with substructure decoupling techniques, which are known to be very sensitive around anti-resonances of the subsystems(s) [4]. Moreover, issues related to observability and controllability at the coupling points are also known to result in and compound decoupling errors [3].

The low-mid-frequency modes in either of the principal directions dominate the response spectrum and belong to the parallel kinematic structure of the mobile machine. The high-frequency modes in the 600 – 1000 Hz range are more local in nature and belong to the spindle assembly. Dynamics of tools and tool-holders would be characterized by local high-frequency modal behaviour and are less affected by the low-frequency structural behaviour. Since the dynamics of the tool and tool holder are specific to the tool and tool holder to be used, these were deliberately neglected from the decoupling scheme. Tool and tool-holder flexibilities are instead recommended to be synthesized with the extracted dynamics at the spindle nose using the RCSA substructure coupling schemes [5-7].

3.1. Sensitivity of extracted dynamics to noise

To emulate measurements, and to investigate the influence of any noise in the measured data on the extracted dynamics, each of the (sub)system FRFs was synthesized with noise having a normal distribution $N(0,1)$, as:

$$h(\omega) = h(\omega)(1 + aN) \quad (12)$$

wherein a represents the level of noise added. In the present case, a high noise level of 30% was added and its influence on the calculated dynamics is compared in Fig. 3. As is evident, though noise results in amplification of some of the high-frequency modes, and a slight underestimation of the low-frequency dynamic stiffness, singularity and/or ill-conditioning of the matrices were not observed presently.

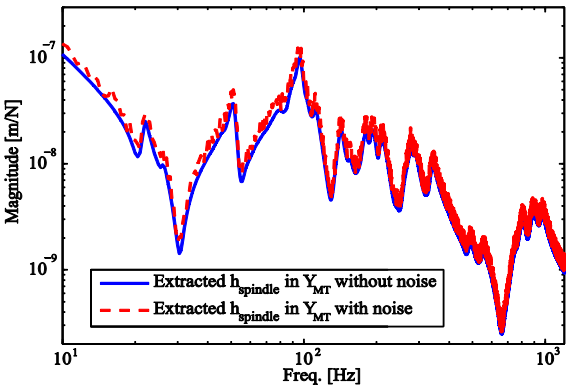

Fig. 3. Comparisons of decoupled machine dynamics (FRFs) at the spindle nose under the influence of simulated noise in FRFs

3.2. Sensitivity of extracted dynamics to changes in the residual substructural base system

To investigate the sensitivity of the calculated dynamics to changes in the substructural base system, two additional base models with different material characteristics were considered. A 'weaker' base was simulated to have a modulus of elasticity half of that of the 'normal' base. A 'stiffer' base on the other hand was simulated to have a density and a modulus of elasticity twice that of the 'normal' base. Any change in the residual substructural base system, i.e. subsystem B, naturally also manifests itself as a change in the assembled AB system characteristics. Hence, new FE models with these new properties were generated for the assembled system as well as for the residual subsystem and a new set of assembled system matrices, i.e. $\boldsymbol{H}^{AB}$ as well as a new set of matrices for the subsystem, i.e. $\boldsymbol{H}^{B}$ were obtained. Eq. (7) was solved separately for each of these base types to extract the response of the machine under these changing influences. Extracted dynamics are compared in Fig. 4.

As evident in Fig. 4, extracted dynamics as observed at the spindle nose shows the low-frequency modes in the 10 – 70 Hz range to be more dependent on the base characteristics than the other high-frequency modes. The mode at ~50 Hz for the 'normal base' shifts to ~42 Hz for the 'weaker base', and similarly shifts to ~59 Hz for the 'stiffer' base. No significant change in dynamic stiffness/flexibilities of these modes was observed. This suggests that a change in the substructural base system(s) has at best a local effect on the extracted dynamics. The dominant machine mode at ~100 Hz is unaffected, as are the other high-frequency modes.

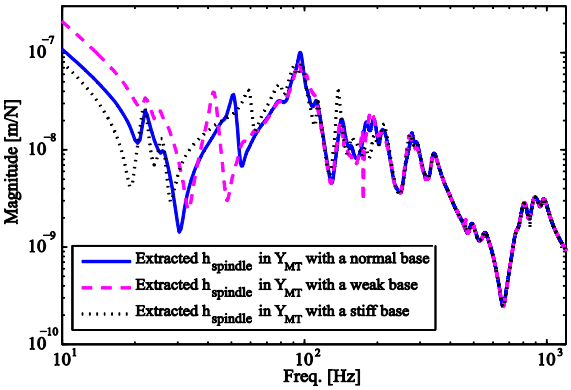

Fig. 4. Comparison of decoupled dynamics (FRFs) at the spindle nose for changing characteristics of the residual substructural base system

4. Conclusions and outlook

This paper has demonstrated that when machine's free-free response cannot be directly determined, it can instead be extracted from known dynamics of the machine assembled onto a base, and from known dynamics of the residual base system. The decoupling scheme was found to be robust even when subjected to vagaries of measurement noise and changes in the residual substructural base system.

The decoupled results can now easily be synthesized with other base models using the previously developed substructure coupling schemes [3, 10] to predict mobile machine tool dynamics prior to moving the machine to a new workpiece and location. This will facilitate first-time right in situ manufacturing of large workpieces.

These simulation based results will guide experimental decoupling that forms part of planned future work.

References

[1] Uriarte L., Zatarian M., Axinte D., et al. Machine tools for large parts. CIRP Annals 2013; 62(2): 731-750.
[2] de Klerk D., Rixen D., Voormeeren S. General framework for dynamic substructuring: History, review and classification of techniques, AIAA Journal 2008; 46(5):1169-1181.
[3] Law M., Rentzsch H., Ihlenfeldt S. Evaluating mobile machine tool dynamics by substructure synthesis. Advanced Materials Research 2014; 1018:373-380.
[4] Voormeeren S., Rixen D. A family of substructure decoupling techniques based on dual assembly approach, Mech. Sys. & Signal Processing 2012; 27:379-396.
[5] Schmitz T., Donaldson R. Predicting high-speed machining dynamics by substructure analysis. CIRP Annals 2000; 49(1): 303-308.
[6] Park S., Altintas Y., Movahhedy M. Receptance Coupling for end mills. Int. J. of Machine Tools and Manufacture 2003; 43:889-896.
[7] Albertelli P., et al. A new receptance coupling substructure analysis methodology to improve chatter free cutting conditions prediction. Int. Journal of Machine Tools and Manufacture 2013; 72:16-24.
[8] Mehrpouya. M., et al. FRF based joint dynamics modeling and identification. Mech. Sys. & Signal Processing 2013; 39:265-279.
[9] D'Ambrogio W., Frefolent A. The role of interface DoFs in decoupling of substructures based on the dual domain decomposition, Mech. Sys. & Signal Processing 2010; 24:2035-2048.
[10] Law M., Rentzsch H., Ihlenfeldt S. Development of a Dynamic Substructuring Framework to Facilitate in Situ Machining Solutions Using Mobile Machine Tools. Proceedia Manufacturing 2015; 1C: 756-767.